

## Thermal Back-Isomerization of Spirocyclic Naphtho-oxazine and Phenanthro-oxazine Derivatives in Alcohols, Nitriles, and Poly(alkyl methacrylates)

by Edgar Völker, Manuela O'Connell, R. Martín Negri, and Pedro F. Aramendía\*

INQUIMAE, Departamento de Química Inorgánica, Analítica y Química Física, Facultad de Ciencias Exactas y Naturales, Universidad de Buenos Aires, Pabellón 2, Ciudad Universitaria, C1428EHA Buenos Aires, Argentina (fax: ++541145763341; e-mail: pedro@qi.fcen.uba.ar)

Dedicated to Professor *André M. Braun* on the occasion of his 60th birthday

---

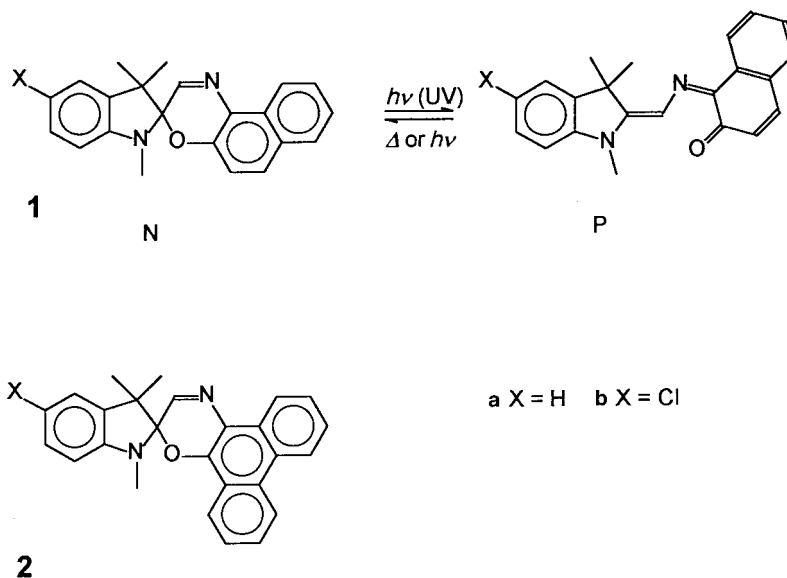
The thermal back-isomerization of spiro[indole-naphtho-oxazine] **1** and spiro[indole-phenanthro-oxazine] **2** was studied in a series of primary alcohols, nitriles, and poly(methylmethacrylate), poly(ethylmethacrylate), and poly(isobutyl methacrylate) films by laser-flash photolysis in the temperature range of 0–70°. The decay is monoexponential in fluid solution, but deviates strongly from this behavior in polymeric environments even above the glass transition temperature of the polymers ( $T_g$ ). In liquids, a very small solvent effect is observed on the isomerization rate constants ( $k_{iso}$ ) for **1**, which is attributed mostly to the solvent viscosity  $\eta$ . The values of  $k_{iso}$  for **2** show influence of solvent viscosity and polarity, which were studied by application of a semiempirical relationship that accounts for non-Markovian processes. The decay kinetics in polymers was described by a *Gaussian* distribution of the activation energy and by a kinetic model that takes into account the simultaneous relaxation of the probe and the environment. For **1** and **2**, the rate constant at the center of the *Gaussian* distribution is very similar to the first-order rate constant in nonpolar solvents. The *Gaussian* width of the distribution ( $\sigma$ ) decreases with temperature and is very similar in all polymers under  $T_g$ , and, above  $T_g$ ,  $\sigma$  decreases more abruptly. We make comparisons of the parameters derived from analysis of both **1** and **2** in polymers, as well as of their behaviors in solution and in polymers.

---

**1. Introduction.** – Spiro-oxazines (SO) are photochromic compounds formed by two heterocyclic parts linked by a common tetrahedral  $sp^3$ -C-atom. The absorption of UV radiation by the thermodynamically stable closed form, N, leads, by cleavage of a C–O bond, to an open structure (*Scheme*). This process occurs in less than 50 ps from the excited singlet state [1]. This photoisomer, P, has extended conjugation and a merocyanine-like structure and, thus, absorbs in the visible region. The open structure, P, sometimes referred to as photomerocyanine, can revert to N thermally or photochemically; thus, P and N form a photochromic system [2][3]. In comparison with other photochromic compounds, some SO compounds are excellent in light-fatigue resistance [4], making them useful in commercial applications such as photochromic lenses and glass plates and photochromic ink [3].

The thermal or dark isomerization involves a large molecular movement, namely a *cis-trans* transformation in the azomethine chain and ring closure. In *cis-trans* isomerizations, it is generally assumed that the activation energy has an electronic contribution and a medium-dependent component, which can be influenced by solvent viscosity, polarity, or both [5–10]. The solvent effects on the thermal back isomerization rate constant,  $k_{iso}$ , were described for the case of sym-

Scheme. Interconversion of the Closed (N) and Open (P) Forms of the Spiro-oxazines



metric carbocyanines and stilbenes according to the so-called semiempirical model [11][12]:

$$k_{\text{iso}} = D \cdot \eta^{-a} \cdot \exp(-E_0/RT) \quad (1)$$

where  $0 \leq a \leq 1$ ,  $D$ , and  $E_0$  are empirically adjustable constants. The departure of the parameter  $a$  from unity is an indication of frequency-dependent friction effects [13].  $E_0$  is considered the medium-independent intrinsic activation energy of the process and is dependent on the molecular structure of the isomerizing molecule. Isoviscosity conditions, obtained by changing solvents in order to maintain constant viscosity while varying temperature, have been applied to determine  $E_0$  values [6].

In comparison to the structurally related spiro-pyran (SP) compounds, SO have faster dark decays. This can be due to the in-plane isomerization pathway of the azomethine chain, not possible in the merocyanine form of SP, in a way similar to what is known for azobenzenes [14][15]. Also in comparison to SP, the merocyanine form of SO can be well-described by a quinoid structure with a small dipolar character [3]. As a consequence,  $k_{\text{iso}}$  values for spiro[indole-naphtho-oxazine] **1** or for spiro[indole-phenanthro-oxazine] **2** display a dependency on solvent polarity opposite to that of SP [16][17].

The photochromic behavior of SP and SO is displayed also in glassy polymer matrices [18][19]. Due to the space required for cyclization, the polymer matrix has a large influence on the kinetics. Unimolecular reactions in polymers usually depart greatly from the monoexponential behavior due to the inhomogeneity of environments in which the reacting molecules are located. This leads to a distribution of rate constants, which is called dispersive kinetics and which can be characterized by a time-

dependent first-order rate constant [20]. Another aspect of reactions carried out in amorphous polymers is that, with increasing temperature, the molecules evolve from a very rigid environment, practically frozen during probe decay, to a liquid-like medium. In between, there is a regime in which probe and environment relax in similar time windows. This has been taken into account in some kinetic analyses [21][22].

The aim of this work is to study the effects of medium on  $k_{\text{iso}}$  for **1** and **2** in alcohols and nitriles, and, for the four compounds shown in the *Scheme*, in poly(alkyl methacrylates). We analyze the viscosity and polarity effects on the decay rate of P in fluids, and the behavior of the kinetics in polymers by distribution and relaxation kinetic analyses. We compare their behaviors in fluid media and in amorphous polymers.

**2. Experimental.** – *Chemicals.* Spiro-oxazines: 2,3-Dihydro-1,3,3-trimethylspiro[indole-2,3'-[3H]naphth[2,1-b][1,4]oxazine (**1a**), 5-chloro-2,3-dihydro-1,3,3-trimethylspiro[indole-2,3'[3H]naphth[2,1-b][1,4]oxazine] (**1b**), 2,3-dihydro-1,3,3-trimethylspiro[indole-2,2'-[2H]phenanthro[9,10-b][1,4]oxazine (**2a**), and 5-chloro-2,3-dihydro-1,3,3-trimethylspiro[indole-2,2'-[2H]phenanthro[9,10-b]oxazine] (**2b**) were used as supplied by Aldrich Chem.

*Solvents:* Alcohols (MeOH, EtOH, PrOH, BuOH, pentanol (PeOH), octanol (OcOH), and decanol (DecOH)) and nitriles (MeCN, propanenitrile, butanenitrile, and pentanenitrile) were anal. or HPLC grade provided by Merck (Argentina), Dorwill (Argentina), or Riedel de-Haën (Switzerland), and were used without further purification. The values for the viscosity and polarity as a function of temp. were obtained from [23].  $\text{CH}_2\text{Cl}_2$  was HPLC grade, freshly distilled and stored over molecular sieves (4 Å).

*Polymers:* Poly(alkyl methacrylates) (poly(methyl methacrylate) (PMMA), poly(ethyl methacrylate) (PEMA), and poly(isobutyl metacrylate) (PIBMA), secondary standards) were purchased from Aldrich and used as received. Molecular weight (Mw), and polydispersity (Mw/Mn) were, resp., 102600 and 2.1 for PMMA, 340000 and 2.7 for PEMA, and 300000 and 2.1 for PIBMA. Glass transition temp. ( $T_g$ ) of the different polymer samples determined in previous work [22] are 103° for PMMA, 61° for PEMA, and 51° for PIBMA.

*Sample Preparation.* Solns. were not degassed and in all cases the concentration was less than  $10^{-5}$  M. Samples in polymer films were prepared as previously described, starting from a  $\text{CH}_2\text{Cl}_2$  soln. of polymer and probe [22]. The SO concentration in the polymer film was always less than 0.5% (w/w). No photochemical or thermal decomposition of the dyes was observed in the temp. range 0–70° during the measurement.

*Absorbance Measurements.* The absorption spectra were recorded on a Shimadzu UV-160A or Shimadzu UV-3101PC spectrophotometer. The solns. were placed in a quartz cuvette of 10 × 10 mm and the polymer films were sandwiched on a brass adapter and placed in a normal cuvette holder. The samples were kept at constant temp. by  $\text{H}_2\text{O}/\text{EtOH}$  circulation with a Lauda RCS 20 thermostat-cryostat. The temp. was measured inside the cuvette or on the polymer-film surface with a Pt100 thermometer. After desired temp. was reached, samples were allowed to relax for at least 4 lifetimes in the dark at each temp. before measurement. Measurements were performed at 0–70° (the maximum temp. range was dependent on the medium). The maximum absorbance of the closed form was 0.1–0.8 units.

*Absorption Coefficients ( $\epsilon$ ) and Equilibrium Constants ( $K_{\text{eq}}$ ).* For **2b**, the absorption coefficient determined in toluene was  $\epsilon^{340}$  (**2b**) =  $5900 \pm 800 \text{ M}^{-1} \text{ cm}^{-1}$ . To determine the concentration in the polymer, a weighed amount of sample was dissolved in toluene, and its absorbance at 340 nm was measured; the contribution of the absorption of the polymer is negligible. The absorption coefficient of the merocyanine form was assumed to be equal to that of **1a**:  $\epsilon^{585}$  (P) =  $68300 \text{ M}^{-1} \text{ cm}^{-1}$  [16]. Equilibrium constants,  $K_{\text{eq}}$ , were calculated from:

$$K_{\text{eq}} = \frac{[\text{P}]}{[\text{N}]} = \frac{A^{585}/\epsilon^{585}}{A^{340}/\epsilon^{340}} \quad (2)$$

In Eqn. 2, it is assumed that the contributions to absorption of P at 340 nm and of N at 585 nm are negligible. If the absorption coefficients used are not correct, the  $K_{\text{eq}}$  is affected by a factor, but there is no influence on the energy difference of the thermochromic equilibrium.

*Flash Photolysis.* The decay of P was followed by laser flash photolysis and absorbance detection at the visible band for time windows shorter than 20 s. Photocoloration was achieved by means of a pulsed Nd:YAG laser (Spectron Lasers, England; 354 nm, 8 ns fwhm, 80 mJ per pulse). The liquid samples were placed in a standard 10 × 10 mm quartz fluorescence cuvette in a thermostatted cuvette holder. Polymer films were placed

in a brass adapter. Further details of the setup are given in [22]. The slower decays (low temp. in polymers, when the total measuring window exceeded 20 s) were recorded in a *Hewlett Packard 8452A* diode array spectrophotometer. In this case, a photography flash with its plastic cover removed served as photolyzing light. Analysis was performed with a *GG420* cut-off filter (*Schott*) to prevent photolysis by the analyzing flash. The temp. was controlled and measured as described above.

**3. Results.** – 3.1. *Absorption Spectrum and Thermochromism.* In the absence of UV excitation, the solutions of **1a** in all solvents are colorless and show three absorption bands in UV region with peaks at 345, 317, and 304 nm, corresponding to the localized  $\pi$  transitions of the two orthogonal parts of the molecule [24]. The positions of the peaks do not change significantly in the different solvents. No absorption of the P form in thermal equilibrium with N was observed in any solvent employed for **1a** across the temperature range investigated, even for the more concentrated solutions. The same is true for the polymer films of **1a** and of **1b**. Thus, we conclude that the spirocyclic naphtho-oxazines studied do not show thermochromic effects in these media.

Solutions of **2a** as well as the polymer films of this compound and of **2b** are colored in the absence of UV radiation at room temperature. An absorption band is observed at *ca.* 600 nm, indicating the presence of the photoisomer in thermal equilibrium with the normal form, which is an important difference with respect to the naphtho compounds. The thermochromism of **1a** has been previously reported [16][22]. Similar behavior was shown by **2b** with a value of  $K_{\text{eq}}$  that is half that of **1a** under the same conditions. A *van't Hoff* representation of  $K_{\text{eq}}$  does not render a straight line in any polymer studied. The slope increases with temperature, as described for **2a** in the same polymers [22]. *Table 1* displays the values of  $K_{\text{eq}}$  of **2b** at various temperatures in PMMA, PEMA, and PIBMA, as well as the calculated energy difference at the higher temperatures measured. If these values correspond to the  $\Delta U$  between N and P (the latter being higher in energy), they are quite similar to the value for **2a** in toluene, for which normal *van't Hoff* behavior is observed [16].

Table 1. *Equilibrium Constant ( $K_{\text{eq}}$ ) for Interconversion of the Closed and Open Forms of 2b in Different Polymers and the Energy Difference ( $\Delta U$ ) of this Reaction (calculated at the higher temperatures measured)*

| PMMA                |                       | PEMA                |                       | PIBMA               |                       |
|---------------------|-----------------------|---------------------|-----------------------|---------------------|-----------------------|
| $T$ [°]             | $K_{\text{eq}}$       | $T$ [°]             | $K_{\text{eq}}$       | $T$ [°]             | $K_{\text{eq}}$       |
| 4.8                 | $5.85 \times 10^{-3}$ | 20.2                | $3.83 \times 10^{-3}$ | 7.2                 | $2.55 \times 10^{-3}$ |
| 17.3                | $6.10 \times 10^{-3}$ | 33.4                | $3.97 \times 10^{-3}$ | 19.7                | $2.58 \times 10^{-3}$ |
| 35.0                | $6.42 \times 10^{-3}$ | 38.4                | $4.01 \times 10^{-3}$ | 32.6                | $2.69 \times 10^{-3}$ |
| 43.9                | $6.63 \times 10^{-3}$ | 46.5                | $4.20 \times 10^{-3}$ | 46.3                | $2.77 \times 10^{-3}$ |
| 52.8                | $6.94 \times 10^{-3}$ | 56.8                | $4.54 \times 10^{-3}$ | 54.7                | $2.92 \times 10^{-3}$ |
| 57.3                | $7.08 \times 10^{-3}$ | 65.7                | $5.19 \times 10^{-3}$ | 63.1                | $3.29 \times 10^{-3}$ |
| 66.8                | $7.60 \times 10^{-3}$ | 70.2                | $5.45 \times 10^{-3}$ | 72.0                | $3.48 \times 10^{-3}$ |
| 74.9                | $8.32 \times 10^{-3}$ | 78.6                | $6.24 \times 10^{-3}$ |                     |                       |
| $\Delta U$ [kJ/mol] |                       | $\Delta U$ [kJ/mol] |                       | $\Delta U$ [kJ/mol] |                       |
| 10.0                |                       | 14.0                |                       | 9.5                 |                       |

In the alcohols, the photoisomer absorption band at the visible region has a maximum of 610–620 nm for **1a** and 590–600 nm for **2a**. In the nitrile solvents, the band is slightly shifted to the blue, with maximum at 590–600 nm for **1a** and 580 for **2a**,

suggesting specific solute-solvent interactions [25]. In polymers, the absorption maxima are similar to those in the nitrile solvents in all cases, reflecting the smaller solvation capacity of the polymers: 590–606 nm for **1a** and **1b**, and 570–580 nm for **2a** and **2b**.

**3.2. Kinetics of the Thermal Decay. Alcohols and Nitriles.** In all cases, mono-exponential back isomerization decays were obtained. The values of  $k_{\text{iso}}$  at 25° are shown in *Table 2*. These values are one order of magnitude smaller for **1a** than for **2a**. That is, the thermal back isomerization is slower for the smaller molecule, suggesting that, at least for one of the compounds, the process is more complex than a diffusional rotation. Additionally, *Table 2* shows that the solvent dependence of  $k_{\text{iso}}$  is different for **2a** and **1a**. In the alcohols,  $k_{\text{iso}}$  decreases with the solvent carbon chain length for **2a**, but no such effect is observed for **1a** for which no clear tendency is observed. Finally, the values of  $k_{\text{iso}}$  are very different in nitrile and alcohol solutions for each molecule, confirming specific solute-solvent interactions. The thermal decays are strongly dependent on temperature (shown in *Fig. 1* for **1a**). Linear *Arrhenius* plots were obtained in all cases. Activation energies,  $E_a$ , and pre-exponential factors,  $A$ , are shown in *Table 2* for the different alcohol and nitrile solvents. While a simple *Arrhenius* law can be questioned for situations in which solvent-solute friction plays a role in determining the reaction rate [9], the parameters of these fits are, nevertheless, quite adequate for prediction of the temperature-dependent isomerization rates for **1a** and **2a** over the whole temperature range examined in this study.

**Polymers.** Contrary to the behavior in solution, in polymers, the decay of the open form departs greatly from the monoexponential kinetics. Also contrary to the behavior in solution, the phenanthro-oxazines decay at a rate 2 to 3 times slower than the naphtho-oxazines.

The decays are analyzed from two different points of view. The first model is a *Gaussian* distribution of activation energy [20], as described by *Eqn. 3*:

$$[P](t) = [P]_0 \frac{1}{\sqrt{2\pi\sigma}} \int \exp\left[-\frac{(E_0 - E)^2}{2\sigma^2} - (v_0 \cdot e - (E_m - E)/RT) \cdot t\right] dE \quad (3)$$

Table 2. Arrhenius Parameters for **1a** and **2a** in Different Solvents. The solvent viscosity ( $\eta$ ), dielectric constant ( $\epsilon$ ), viscosity activation energy ( $E_\eta$ ), and thermal back-isomerization rate constant ( $k_{\text{iso}}$ ) for **1a** and **2a** at 25° are also indicated.

| Solvent        | $\eta$ [cP] | $E_\eta$ [kJ/mol] | $\epsilon$ | <b>2a</b>      |                  |                                     | <b>1a</b>      |                  |                                     |
|----------------|-------------|-------------------|------------|----------------|------------------|-------------------------------------|----------------|------------------|-------------------------------------|
|                |             |                   |            | $E_a$ [kJ/mol] | $\ln [A/s^{-1}]$ | $k_{\text{iso}}$ [s <sup>-1</sup> ] | $E_a$ [kJ/mol] | $\ln [a/s^{-1}]$ | $k_{\text{iso}}$ [s <sup>-1</sup> ] |
| MeOH           | 0.6         | 10.4              | 34         | 70 ± 1         | 30.1 ± 0.7       | 5.3                                 | 73 ± 3         | 29.0 ± 1.0       | 0.40                                |
| EtOH           | 1.3         | 15.7              | 26         | 73 ± 3         | 30.9 ± 1.0       | 4.3                                 | 74 ± 2         | 29.4 ± 0.7       | 0.49                                |
| PrOH           | 1.9         | 17.8              | 22         | 73 ± 2         | 30.9 ± 0.7       | 4.3                                 | 74 ± 2         | 29.6 ± 0.7       | 0.37                                |
| BuOH           | 2.5         | 19.5              | 19         | 70 ± 1         | 29.8 ± 0.5       | 3.8                                 | 77 ± 2         | 30.5 ± 0.7       | 0.55                                |
| PeOH           | 3.7         | 21.8              | 14         | 71 ± 2         | 30.0 ± 0.7       | 2.8                                 | 79 ± 2         | 31.4 ± 0.7       | 0.45                                |
| OcOH           | 7.5         | 24.1              | 11         | 64 ± 2         | 27.0 ± 0.8       | 2.1                                 | 79 ± 3         | 31.1 ± 0.9       | 0.53                                |
| DecOH          | 11.0        | 26.4              | 8          | 61 ± 2         | 25.7 ± 0.6       | 1.9                                 | 80 ± 3         | 31.5 ± 0.6       | 0.40                                |
| MeCN           | 0.3         | 38                | 37         | 68 ± 1         | 28.3 ± 0.3       | 1.7                                 | 75 ± 1         | 30.9 ± 0.4       | 0.67                                |
| Propanenitrile | 0.3         |                   | 30         | 64 ± 2         | 26.1 ± 0.7       | 1.0                                 | 69 ± 2         | 28.7 ± 0.8       | 0.89                                |
| Butanenitrile  | 0.6         |                   | 25         | 63 ± 1         | 25.8 ± 0.3       | 1.7                                 | 60 ± 4         | 24.0 ± 1.0       | 0.78                                |
| Pentanenitrile |             |                   | 20         | 66 ± 2         | 26.3 ± 0.9       | 1.7                                 | 73 ± 1         | 29.5 ± 0.3       | 0.94                                |

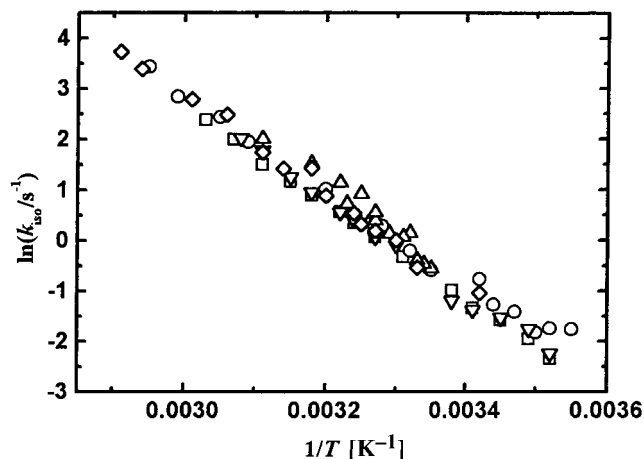


Fig. 1. Temperature dependence of  $k_{\text{iso}}$  for **1a** in different solvents: ( $\Delta$ ) MeOH, ( $\circ$ ) EtOH, ( $\diamond$ ) PrOH, ( $\nabla$ ) PeOH, and ( $\square$ ) DecOH

In Eqn. 3,  $[P]_0$  represents the initial merocyanine concentration,  $E$  is the energy of the probe in its ground state,  $E_m$  is the energy of the maximum of the energy barrier,  $\nu_0$  is an energy-independent frequency factor, and  $\sigma$  and  $E_0$  represent the width and the value of the energy at the center of the ground-state energy distribution. The rate constant at  $E = E_0$ ,  $k(E_0) = \nu_0 \cdot \exp[-(E_m - E_0)/RT]$  and  $\sigma$  are the kinetic parameters that are fitted in each decay. Results of these parameters as a function of temperature are shown for **2b** in the three polymers and for the four probes in PEMA in Fig. 2. These are typical results:  $k(E_0)$  is equal, within experimental error, in the three polymers across the entire temperature range. For **1a** and **2a**,  $k(E_0)$  is also very similar to the value of the first-order-decay rate constant measured in toluene [16]. We have no values in toluene for the other two spiro-oxazines. The values of  $\sigma$  are also very similar in all polymers in the glassy state, and they are temperature-independent within experimental error. As a consequence, the decays are almost equal in all polymers when the three are under the  $T_g$ . Above the  $T_g$ ,  $\sigma$  decreases but its values is still comparable to  $kT$ , so the decay does not reach the monoexponential behavior. According to this kinetic model, the only influence of the polymer matrix on the decay kinetics is the microheterogeneity of environments of different activation energies provided by the network.

The other kinetic model used assumes a simultaneous relaxation of the probe and the matrix [26]. The relaxation of the matrix is assumed to be single exponential with a lifetime  $\tau_m$ . This relaxation is assumed to stabilize the probe in its environment. As a consequence of this relaxation, the decay probability of the probe decreases from an initial value  $k_0$  to a final value  $k_\infty$ . The time-dependent-decay probability,  $k(t)$ , of the probe is assumed to be given by Eqn. 4:

$$k(t) = k_\infty + (k_0 - k_\infty) \exp(-t/\tau_m) \quad (4)$$

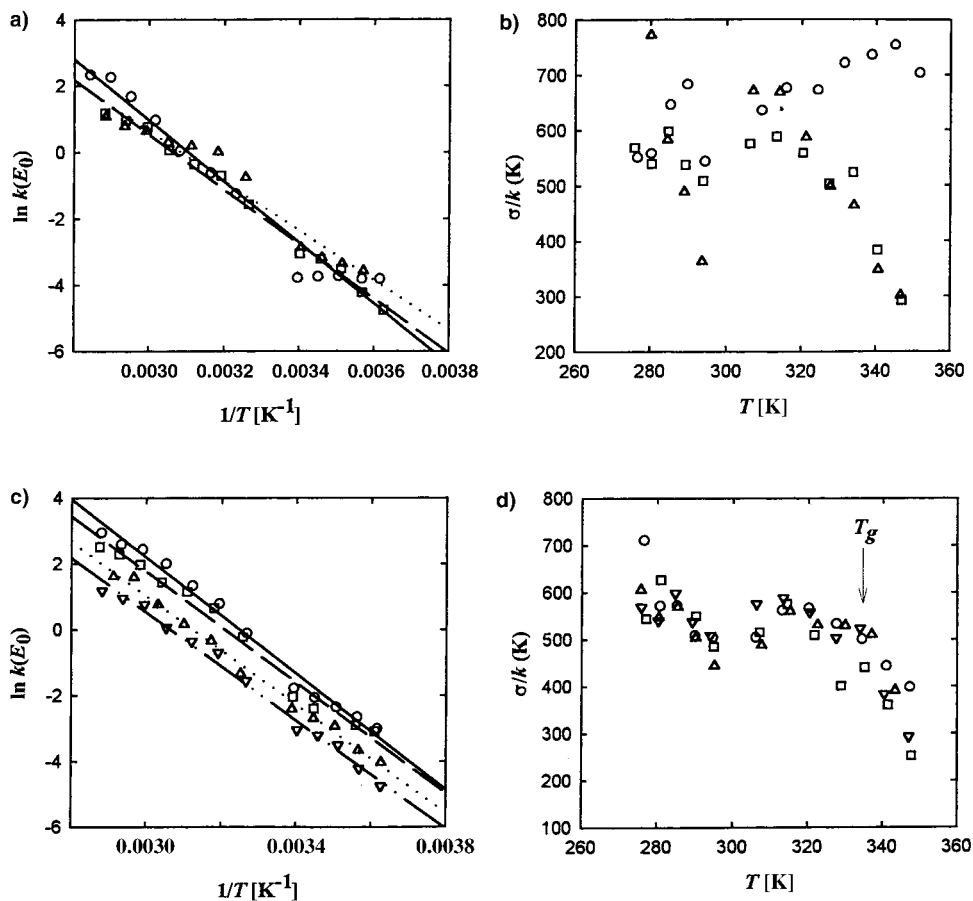


Fig. 2. Temperature dependence of the kinetic parameters of the Gaussian distribution (Eqn. 3 and accompanying text). a) The rate constant ( $k(E_0)$ ) at the center of the distribution and b) the standard deviation ( $\sigma$ ), for **2b** in PMMA ( $\circ$  and full line), PEMA ( $\square$  and dashed line), and PIBMA ( $\triangle$  and dotted line); c)  $k(E_0)$  and d)  $\sigma$  in PEMA for **1a** ( $\circ$  and full line), **1b** ( $\square$  and dashed line), **2a** ( $\triangle$  and dotted line), and **2b** ( $\nabla$  and dashed-dotted line); rate constants in  $s^{-1}$ .

This time dependence of the decay probability renders a time dependence for  $[P](t)$ , which is:

$$[P](t) = [P]_0 \exp \{ -k_\infty t - [k_0 - k_\infty] \tau_m [1 - \exp(-t/\tau_m)] \} \quad (5)$$

The fit of the decay curves to Eqn. 5 are better at higher temperatures, as judged by the magnitude of the mean-square deviation from measured and fitted values and from the time distribution of the difference between the same values. Arrhenius plots of the kinetic parameters of Eqn. 5:  $k_0$ ,  $k_\infty$ , and  $\tau_m$  are shown in Fig. 3 for **1a**. Arrhenius parameters for these rate coefficients as well as for  $k(E_0)$  are given in Table 3 for all probes in the three polymers.

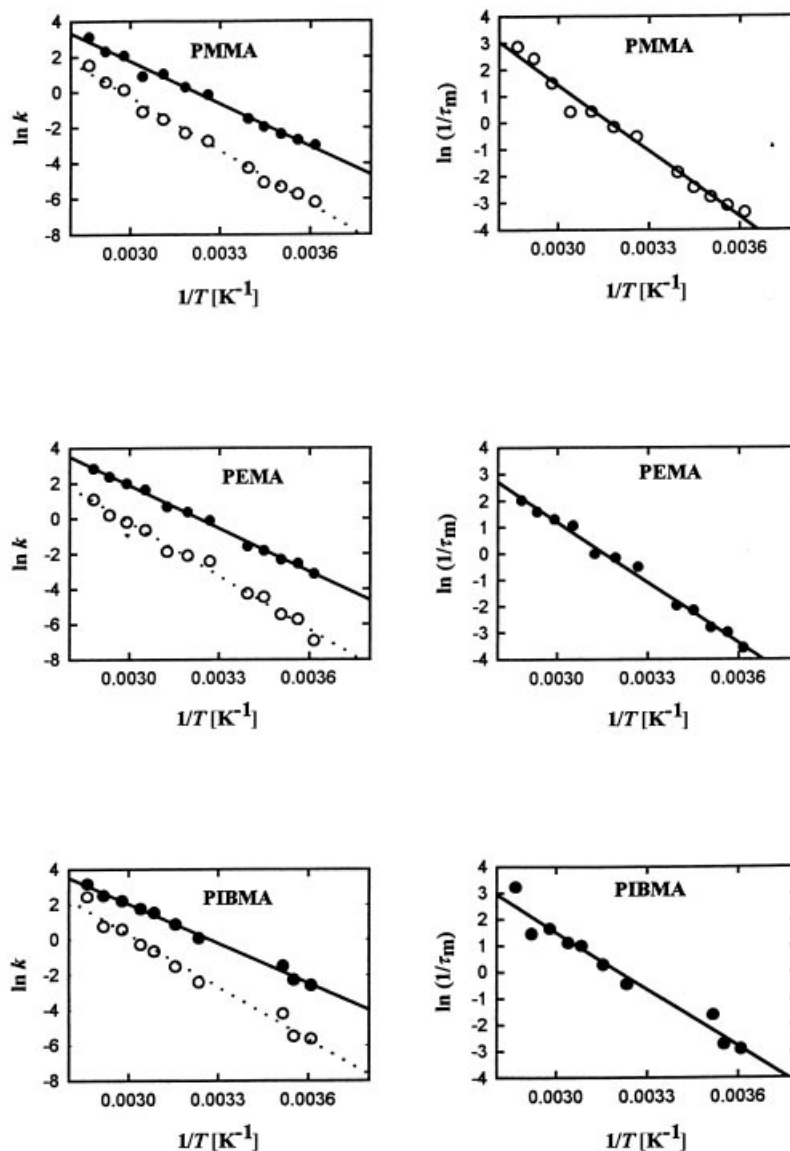


Fig. 3. Arrhenius plots for the three kinetic parameters of Eqn. 5 for **1a** in PMMA, PEMA, and PIBMA. Left-side plots:  $k_0$  (● and full line) and  $k_\infty$  (○ and dotted line). Right-side plots:  $1/\tau_m$ . Rate constants and  $1/\tau_m$  in  $\text{s}^{-1}$ .

As expected, activation energies of  $k_\infty$  are greater than the corresponding values for  $k_0$ , reflecting the stabilization energy provided by matrix relaxation. The Arrhenius slope of  $\tau_m$  corresponds to the energy required for matrix movement. These are very similar for all probes in the same polymer, indicating, as expected, that the type of movement responsible for matrix relaxation is of the same nature for all probes. A stretched exponential decay of the form:



Table 3. Arrhenius Parameters for  $k(E_0)$  (Eqn. 3) and  $k_0$ ,  $k_\infty$ , and  $\tau_m$  (Eqn. 5) for **1a**, **1b**, **2a**, and **2b** in the Three Polymers.

| Probe     | Polymer |                       | $k(E_0)$       | $k_0$          | $k_\infty$     | $1/\tau_m$     |
|-----------|---------|-----------------------|----------------|----------------|----------------|----------------|
| <b>1a</b> | PMMA    | $E_a$ [kJ/mol]        | $66 \pm 6$     | $66 \pm 2$     | $84 \pm 2$     | $68 \pm 3$     |
|           |         | $\log A$ [ $s^{-1}$ ] | $11.0 \pm 0.9$ | $11.2 \pm 0.2$ | $13.0 \pm 0.4$ | $11.3 \pm 0.5$ |
|           | PEMA    | $E_a$ [kJ/mol]        | $73 \pm 3$     | $68 \pm 1$     | $84 \pm 3$     | $63 \pm 2$     |
|           |         | $\log A$ [ $s^{-1}$ ] | $12.4 \pm 0.5$ | $11.4 \pm 0.2$ | $13.1 \pm 0.5$ | $10.4 \pm 0.3$ |
|           | PIBMA   | $E_a$ [kJ/mol]        | $63 \pm 3$     | $62 \pm 2$     | $83 \pm 4$     | $60 \pm 4$     |
|           |         | $\log A$ [ $s^{-1}$ ] | $10.8 \pm 0.4$ | $10.7 \pm 0.3$ | $13.1 \pm 0.7$ | $10.0 \pm 0.7$ |
| <b>1b</b> | PMMA    | $E_a$ [kJ/mol]        | $70 \pm 5$     | $65 \pm 1$     | $73 \pm 2$     | $62 \pm 1$     |
|           |         | $\log A$ [ $s^{-1}$ ] | $11.9 \pm 0.8$ | $10.9 \pm 0.2$ | $11.1 \pm 0.4$ | $10.3 \pm 0.3$ |
|           | PEMA    | $E_a$ [kJ/mol]        | $70 \pm 3$     | $68 \pm 1$     | $85 \pm 3$     | $66 \pm 2$     |
|           |         | $\log A$ [ $s^{-1}$ ] | $11.7 \pm 0.5$ | $11.6 \pm 0.3$ | $13.4 \pm 0.5$ | $11.1 \pm 0.3$ |
|           | PIBMA   | $E_a$ [kJ/mol]        | $64 \pm 4$     | $61 \pm 3$     | $77 \pm 4$     | $58 \pm 3$     |
|           |         | $\log A$ [ $s^{-1}$ ] | $10.8 \pm 0.7$ | $10.4 \pm 0.5$ | $12.0 \pm 0.7$ | $9.7 \pm 0.6$  |
| <b>2a</b> | PMMA    | $E_a$ [kJ/mol]        | $72 \pm 3$     | $62 \pm 1$     | $64 \pm 2$     | $59 \pm 2$     |
|           |         | $\log A$ [ $s^{-1}$ ] | $12.0 \pm 0.5$ | $10.2 \pm 0.2$ | $9.4 \pm 0.3$  | $9.5 \pm 0.3$  |
|           | PEMA    | $E_a$ [kJ/mol]        | $68 \pm 2$     | $59 \pm 1$     | $67 \pm 3$     | $51 \pm 3$     |
|           |         | $\log A$ [ $s^{-1}$ ] | $11.2 \pm 0.3$ | $9.7 \pm 0.3$  | $9.9 \pm 0.5$  | $8.1 \pm 0.5$  |
|           | PIBMA   | $E_a$ [kJ/mol]        | $64 \pm 6$     | $61 \pm 5$     | $79 \pm 3$     | $55 \pm 6$     |
|           |         | $\log A$ [ $s^{-1}$ ] | $10.4 \pm 1.0$ | $10.1 \pm 0.8$ | $12.2 \pm 0.5$ | $8.9 \pm 1.0$  |
| <b>2b</b> | PMMA    | $E_a$ [kJ/mol]        | $76 \pm 5$     | $61 \pm 2$     | $65 \pm 3$     | $57 \pm 3$     |
|           |         | $\log A$ [ $s^{-1}$ ] | $12.4 \pm 0.8$ | $9.8 \pm 0.4$  | $9.4 \pm 0.6$  | $9.0 \pm 0.5$  |
|           | PEMA    | $E_a$ [kJ/mol]        | $68 \pm 2$     | $64 \pm 2$     | $77 \pm 3$     | $61 \pm 4$     |
|           |         | $\log A$ [ $s^{-1}$ ] | $10.9 \pm 0.3$ | $10.4 \pm 0.4$ | $11.6 \pm 0.5$ | $9.7 \pm 0.6$  |
|           | PIBMA   | $E_a$ [kJ/mol]        | $62 \pm 5$     | $58 \pm 4$     | $73 \pm 5$     | $51 \pm 6$     |
|           |         | $\log A$ [ $s^{-1}$ ] | $10.0 \pm 0.8$ | $9.4 \pm 0.7$  | $11.1 \pm 0.9$ | $8.3 \pm 1$    |

$$[P](t) = [P]_0 \cdot \exp[-(t/\tau)^\alpha] \quad (6)$$

with  $1 \geq \alpha > 0$ , was used to describe the decay in polymers in many cases [27–29]. The success of the stretched exponential is due to the inclusion of a broad spectrum of relaxation times (which broadens as  $\alpha$  decreases). Its drawbacks are a lack of physical insight into the process and uncertainty in the fitting procedure derived from the prediction of a divergence decay probability as  $t \rightarrow 0$ . In previous work [26], we compared the decay of SP described by the stretched exponential and by Eqn. 5. Taking into account this work and the previous discussion, we do not expect new insights into the process from a decay analysis based on the stretched exponential, and we restrict the kinetic analysis to Eqns. 3 and 5.

**4. Discussion.** – *Alcohol and Nitrile Solvents.* First we shall analyze the case of **1a**, for which there is no discernable tendency in the values of  $k_{\text{iso}}$  at a fixed temperature through a given series of solvents. However, the values of  $E_a$  show a slight but systematic increase with the solvent carbon chain length, which is coincident with the prediction of a frictional-diffusion model where macroscopic viscosity  $\eta$  is the friction parameter.

To investigate possible solvent effects on  $E_a$ , isoviscosity plots were constructed for different fixed viscosities. In all cases, linear isoviscosity plots were obtained (Fig. 4). This indicates that nonspecific solvent effects, if any, must be due in a first

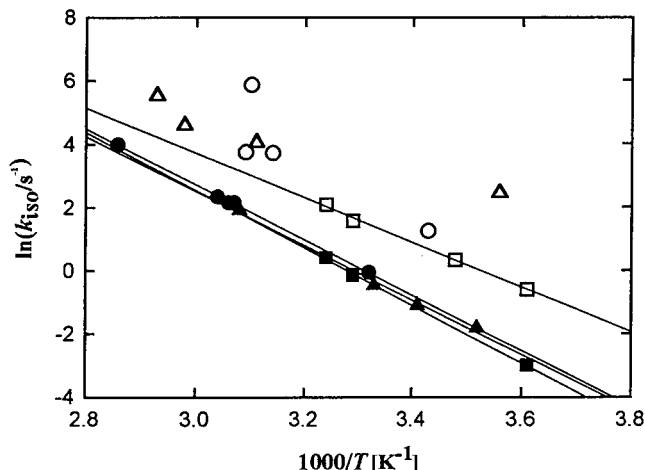


Fig. 4. Isoviscosity graphs for **1a**: 1 cP (●), 3 cP (▲), 5 cP (■), and for **2a**: 1 cP (○), 5 cP (□), 7 cP (△). For **2a** at 1 cP and 7 cP, no linear correlations are drawn.

approximation to viscous friction, but not to solvent polarity or other effects. The slopes of the isoviscosity plots are very similar, rendering energy values of 71–75 kJ/mol. If the model given by Eqn. 1 is assumed, these values should be an estimation of the electronic contribution,  $E_0$ .

The parameter  $a$  can be estimated by considering the normal viscosity-temperature dependence:

$$\eta = \eta_0 \exp(E_\eta/RT) \quad (7)$$

where  $\eta_0$  and  $E_\eta$  are constants for each solvent. If we replace  $\eta$  as given by Eqn. 7 in Eqn. 1, then an Arrhenius behavior for  $k_{\text{iso}}$  is predicted with activation energy  $E_a$  given by:

$$E_a = E_0 + a \cdot E_\eta \quad (8)$$

Eqn. 8 allows us to estimate the value of  $a$ , the parameter that accounts for the viscosity dependence of  $k_{\text{iso}}$  in the frame of Eqn. 1, from the slope of the  $E_a$  vs.  $E_\eta$ . We obtained  $E_0 = 67 \pm 2$  kJ/mol and  $a = 0.48 \pm 0.08$ . It is observed that the value of  $a$  is far from the unity, indicating that the system undergoes a non-Markovian process, reflecting also that the solvent effects on  $k_{\text{iso}}$  are very small.

We will now discuss the back isomerization of **2a**. For this spiro-oxazine,  $k_{\text{iso}}$  decreases with the length of the alcohol carbon chain, indicating that a viscous friction effect can be present. However, the activation energy of  $k_{\text{iso}}$  does not follow this tendency. The values of  $E_a$  remain almost constant and a small decrease is observed for OcOH and DecOH (Fig. 5), which is very different from the behavior observed for **1a**. Moreover, the isoviscosity curves (Fig. 4) are more dispersed for **2a** than for **1a**. These results cannot be explained with a model that considers the viscous friction as the only

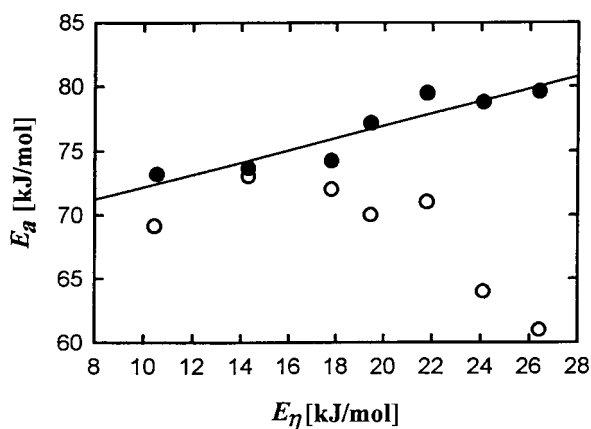


Fig. 5. Activation energy,  $E_a$ , of  $k_{\text{iso}}$  as a function of  $E_\eta$  (Eqn. 8) for **1a** (●) and **2a** (○, with no correlation drawn).

nonspecific solvent effect. Hence, we explored the possibility of polarity influence on  $k_{\text{iso}}$  for **1a**, by considering a modification of the empirical model to take into account the effect of solvent viscosity and polarity on the activation energy [30]:

$$k_{\text{iso}} = \frac{D}{\eta^a} \exp \left[ - (E_0 - E_1/\varepsilon)/RT \right] \quad (9)$$

where  $E_1/\varepsilon$  takes into account polarity effects. In this model, the explicit dependence of the solvent viscosity is kept the same as in Eqn. 1, but the polarity effects on the activation are introduced with an additional term. We have performed different fits of  $k_{\text{iso}}$  to Eqn. 9, where  $\eta$  and  $\varepsilon$  are the variables, and  $D$ ,  $E_0$ ,  $a$ , and  $E_1$  the fitting parameters. The fits were performed under different conditions, e.g. with  $D$ ,  $E_0$ ,  $a$ , and  $E_1$  as freely adjustable parameters, or keeping constant alternatively, the parameters  $D$ ,  $E_0$ , or  $a$ . For every case, the fits were performed with the data of  $k_{\text{iso}}$  grouped in two sets and compared. One set included all the data for  $k_{\text{iso}}$  obtained for all the alcohols at the different temperatures, and another set included values for each individual solvent. The best fits were obtained when the constraint  $E_1 = E_0$  was applied to the complete set of  $k_{\text{iso}}$  values. In that case, the recovered values of the parameters were  $E_1 = E_0 = 55 \pm 5$  kJ/mol and  $a = 0.4 \pm 0.1$ .

According to Eqn. 9, the experimental activation energy  $E_a = -R \cdot d \ln(k_{\text{iso}})/d(1/T)$ , keeping the constraint  $E_1 = E_0$ , is given by:

$$E_a = E_0 \left[ 1 - \frac{1}{\varepsilon} \right] + a \cdot E_\eta - \frac{E_0}{\varepsilon^2} \cdot T \cdot \frac{d\varepsilon}{dT} \quad (10)$$

As the first term of the Eqn. 10 makes the major contribution to  $E_a$ , the model explains qualitatively two experimental observations, the decrease in activation energy with the solvent carbon-chain length and the deviation of the isoviscosity plots from linearity.

Although the model is very crude, the results obtained show that it is necessary to consider not only the viscous interaction but also the medium polarity effect on the dark isomerization of **2a**. It is concluded that, as  $E_a$  decreases when  $\varepsilon$  increases, the transition state must be more polar than P.

The values of  $k_{\text{iso}}$  at a fixed temperature, as well as the values of  $E_a$  and  $A$  are different for the series of nitriles compared to the alcohols. The activation energies and pre-exponential factors listed in *Table 1* differ for alcohols and nitriles of similar viscosity and polarity. No trends in the behavior of  $k_{\text{iso}}$  and  $E_a$  were found for the spirooxazines in nitriles. The different behavior in two series of solvents is not unexpected as it has been observed for the isomerization of related compounds [31]. Moreover, that the solvent effects are much less in nitrile solution than in alcohol solution can be related to the lower intensity of the solvation interactions expected for the nitriles.

*Polymers.* The thermochromic behavior can be qualitatively explained when a *Gaussian* distribution of energy differences between the open and closed forms in equilibrium (characterized by a central value  $\Delta E_0$  and a distribution width  $\sigma$ ) is assumed. This is similar to the assumptions made in the analysis of the decay kinetics of the open form by the *Gaussian*-distribution model. If this equilibrium energy-difference-distribution function is centered in a value similar to the slope of the *van't Hoff* plots at high temperature, then the existence of states of lower energy difference causes the equilibrium constant to decrease more slowly as the temperature is lowered. This is in agreement with the observed tendency of  $K_{\text{eq}}$ . Such a model was used to describe the thermochromism of **2a** in the poly(alkyl methacrylates) [22].

The equilibrium constants can be correctly reproduced with values of  $\Delta E_0$  similar to the ones in solution and values of  $\sigma$  similar to those of the kinetic decays under comparable conditions. Nevertheless, the fitting procedure does not show neat convergence to a single set of values. This can be due to an inadequate amount of data, the need for four fitting parameters (see *Eqn. 10* of [22]), and the limited temperature range of the observation. Consequently, no new information can be obtained in this way.

If the quality of the fits of the kinetic data to the two models used is compared, the *Gaussian*-distribution model is favored. It describes very well the decays over the whole temperature range. The relaxation model is as good at the higher temperatures, as expected, because the relaxation model does not take into account the heterogeneity of the polymer, and because the values of its kinetic parameters are mean values. These may not represent adequately the actual situation at lower temperatures, where the distribution is broader, and thus it is more important to consider it explicitly.

If the kinetic parameters derived from both models are compared, in general it is seen that  $k(E_0)$  and  $k_0$  have very similar values, whereas  $k_\infty$  is 10–20 times smaller. The values of  $\tau_m$  are such that relaxation is always completed in the time window of the decay. The average activation energy of  $k_0$  is  $63 \pm 3$  kJ/mol and of  $k_\infty$  is  $76 \pm 8$  kJ/mol, considering all probes and polymers as given in *Table 3*. The difference in activation energy between these two rate constants can be taken as the stabilization energy of the merocyanine form caused by matrix relaxation; this value is  $13 \pm 6$  kJ/mol, as an overall average. The largest values correspond to PIBMA, the softest polymer with  $18 \pm 3$  kJ/mol as average for the four probes, while the smallest values correspond to PMMA and

the phenanthro-oxazines, the combination of the greatest probes and the hardest polymer with  $3 \pm 1$  kJ/mol.

The activation energy of  $\tau_m$  is  $59 \pm 5$  kJ/mol considering all probes and polymers. The averages are  $62 \pm 5$  kJ/mol for PMMA,  $60 \pm 7$  kJ/mol for PEMA, and  $56 \pm 4$  kJ/mol for PIBMA. Though these values are in the range expected according to the  $T_g$  value of the polymers, the difference is quite small and within the magnitude of uncertainties. Neater is the separation between the naphtho- and the phenanthro-oxazines when they are considered separately. For **1a** and **1b**, the activation energy of  $\tau_m$  is  $63 \pm 4$  kJ/mol and for **2a** and **2b**,  $56 \pm 5$  kJ/mol. Nevertheless, the value of the average activation energy of  $\tau_m$ , together with the *Arrhenius* behavior of all kinetic parameters, indicated that the isomerization of SO is not controlled by the extended movements of the polymer backbone responsible for the glass-rubber transition. On the contrary, they seem to be dependent on more local movements that have activation energies on the order of 80 kJ/mol in poly(alkyl methacrylates) [32].

The smaller values of  $k(E_0)$  and  $k_0$  for **2a** and **2b** compared to **1a** and **1b** can be attributed to the greater size of the former two compounds. Nevertheless the volume difference is not so great: **1a** has a volume of  $300 \text{ \AA}^3$  [33];  $20 \text{ \AA}^3$  must be added for a Cl substituent and  $43 \text{ \AA}^3$  for a condensed benzene ring. This renders a 20% volume increase from **1a** to **2b**. Considering that there is no energetic difference in  $k(E_0)$  and  $k_0$  between naphtho- and phenanthro-oxazines, the smaller rate constants must be attributed to the frequency factors determined by entropic effects that can arise from the greater volume requirements of **2a** and **2b**.

The relaxation view of the kinetics, though not so accurate across the whole temperature range as the *Gaussian* distribution model, gives meaningful parameters and another insight into the isomerization process and its interaction with the medium.

**Conclusions.** – The solvent influence on spirooxazines is much less than for the related spiropyrans. This can be due to the low polarity of its quinoid structure and to the greater stability of the open form isomer (*trans-trans-cis* in the azomethine chain [3]) that requires a small displacement of the two cycles to rebuild the C–O bond of the spiro closed form.

The dark isomerization decay in organic solvents at a fixed temperature is slower for **1a** than for **2a**. The main solvent influence on  $k_{iso}$  for **1a** is due to the viscous friction. In the case of **2a** there is other solvent effect, besides the viscous friction, as it is seen from the solvent dependence of  $E_a$ . We explain this effect by taking into account the solvent polarity and conclude that the transition state is more polar than P, the open form of **2a**.

On the other hand, the dark kinetics in polymers is faster for **1a** than for **2a**, contrary to the behavior in organic solvents. As the values of  $E_a$  are very similar in both media, the difference can be assigned to entropic factors. These are probably related to the larger volume of **2a** with respect to **1a** (ca. 20%), which is expected to influence the isomerization in the more rigid polymer matrixes.

*R. M. N.* and *P. F. A.* are research staff of CONICET (Consejo Nacional de Investigaciones Científicas y Técnicas, Argentina). *M. O. C.* thanks ANPCyT (Agencia Nacional de Promoción de la Ciencia y la Técnica, Argentina) for a fellowship. The work was performed with support from ANPCyT (PICT 4438), CONICET (PIA 0388), and the Universidad de Buenos Aires (grant TW10).

## REFERENCES

- [1] F. Wilkinson, D. R. Worrall, J. Hoble, L. Jansen, L. Williams, A. J. Langley, P. J. Matousek, *J. Chem. Soc., Faraday Trans.* **1996**, *92*, 1331.
- [2] R. Guglielmetti, in 'Photochromism Molecules and Systems', Ed. H. Dürr, H. Bouas-Laurent, Elsevier, Amsterdam, 1990, p. 314–466.
- [3] S. Maeda, in 'Organic Photochromic and Thermochromic Compounds', Ed. J. C. Crano, R. J. Guglielmetti, Plenum Press, New York, 1999, Vol. 1, p. 85–109.
- [4] G. Baillet, G. Giusti, R. Guglielmetti, *J. Photochem. Photobiol., A* **1993**, *70*.
- [5] J. Jaraudias, *J. Photochem.* **1980**, *13*, 35.
- [6] S. P. Velsko, G. R. Fleming, *Chem. Phys.* **1982**, *65*, 59.
- [7] G. Pontorini, F. Momicchioli, *Chem. Phys.* **1991**, *151*, 111.
- [8] J. E. I. Korppi-Tommola, A. Hakkarainen, T. Hukka Subbi, *J. Phys. Chem.* **1991**, *95*, 8482.
- [9] H. A. Kramers, *Physica* **1940**, *7*, 284.
- [10] P. F. Aramendia, R. M. Negri, E. San Román, *J. Phys. Chem.* **1994**, *98*, 3165.
- [11] Y.-P. Sun, J. Saltiel, *J. Phys. Chem.* **1989**, *93*, 8310.
- [12] D. Gegiou, K. A. Muszkat, E. Fischer, *J. Am. Chem. Soc.* **1968**, *90*, 12.
- [13] B. Bagchi, D. W. Oxtoby, *J. Chem. Phys.* **1983**, *78*, 2735; B. Bagchi, G. R. Fleming, D. W. Oxtoby, *J. Phys. Chem.* **1983**, *78*, 7375.
- [14] R. G. Weiss, *Tetrahedron* **1988**, *44*, 3413.
- [15] H. Rau, in 'Photochromism. Molecules and Systems', Ed. H. Dürr, H. Bouas-Laurent, Elsevier, Amsterdam, 1990, p. 165–192.
- [16] G. Favaro, F. Masetti, U. Mazzucato, G. Ottavi, P. Allegrini, V. Malatesta, *J. Chem. Soc., Faraday Trans.* **1994**, *90*, 333.
- [17] Y. Sueishi, M. Ohcho, N. Nishimura, *Bull. Chem. Soc. Jpn.* **1985**, *58*, 2608.
- [18] V. A. Krongauz, in 'Photochromism. Molecules and Systems', Ed. H. Dürr, H. Bouas-Laurent, Elsevier, Amsterdam, 1990, p. 793–821.
- [19] K. Ichimura, in 'Organic Photochromic and Thermochromic Compounds', Ed. J. C. Crano, R. J. Guglielmetti, Plenum Press, New York, 1999, Vol. 2, p. 9–63.
- [20] R. Richert, *Chem. Phys. Lett.* **1985**, *118*, 534; W. J. Albery, P. N. Bartlett, C. P. Wilde, J. R. Darwent, *J. Am. Chem. Soc.* **1985**, *107*, 1854.
- [21] R. Richert, *Chem. Phys.* **1988**, *122*, 455.
- [22] M. Levitus, P. F. Aramendia, *J. Phys. Chem., B* **1999**, *103*, 1864.
- [23] Landolt-Börnstein, 'Zahlenwerte und Funktionen', Springer, Berlin, 1967, Band II, Teil 5.
- [24] D. A. Reeves, F. Wilkinson, *J. Chem. Soc., Faraday Trans. 2* **1973**, *69*, 1381.
- [25] G. Favaro, F. Ortica, V. Malatesta, *J. Chem. Soc., Faraday Trans.* **1995**, *91*, 4099.
- [26] M. Levitus, M. Talhavini, R. M. Negri, T. D. Z. Atvars, P. F. Aramendia, *J. Phys. Chem., B* **1997**, *101*, 7680.
- [27] K. Horie, I. Mita, *Adv. Polym. Sci.* **1989**, *88*, 77.
- [28] J. Klafter, A. Blumen, *Chem. Phys. Lett.* **1985**, *119*, 377.
- [29] T. Tsutsui, A. Hatakeyama, S. Saito, M. Irie, *Chem. Phys. Lett.* **1986**, *132*, 563.
- [30] R. M. Anderton, J. F. Kauffman, *J. Phys. Chem.* **1994**, *98*, 1125.
- [31] Y. Onganer, M. Yin, D. R. Bessire, E. L. Quitevis, *J. Phys. Chem.* **1993**, *97*, 2344.
- [32] N. G. McCrum, B. E. Read, G. Williams, in 'Anelastic and Dielectric Effects in Polymeric Solids', Dover Publications, Inc., New York, 1967.
- [33] J. T. Edwards, *J. Chem. Educ.* **1970**, *47*, 261.

Received June 11, 2001